Polymer Degradation and Stability 133 (2016) 255–263

Contents lists available at ScienceDirect

Polymer Degradation and Stability

journal homepage: www.elsevier.com/locate/polydegstab

Water diffusion and swelling stresses in highly crosslinked epoxy matrices

Andrea Toscano, Giuseppe Pitarresi*, Michele Scafidi, Maria Di Filippo, Giuseppe Spadaro, Sabina Alessi

Università degli Studi di Palermo, Dipartimento di Ingegneria Chimica, Gestionale, Informatica, Meccanica (DICGIM), Viale delle Scienze, 90128 Palermo, Italy

ARTICLE INFO

Article history:
Received 18 May 2016
Accepted 2 September 2016
Available online 7 September 2016

Keywords:
Epoxy resin
Hydrothermal aging
Swelling
Dynamic Mechanical Thermal Analysis
Photoelastic Stress Analysis

ABSTRACT

The present work investigates the swelling induced stresses arising in two epoxy systems during water uptake. The analysed systems are two epoxy resin based on DGEBA monomer and DGEBF monomer respectively, both fully cured by DDS amine. The systems achieve different cross-link density degrees, and are characterised by high glass transition temperatures ranging between 200 and 230 °C. Both epoxies have been conditioned in deionized water baths at two different temperatures (50 °C and 80 °C). A desorption process at room temperature in a dry airborne environment was performed after saturation. Dynamic Mechanical Thermal Analysis, carried out at the various stages of hydrothermal conditioning, has allowed to characterise the modifications occurring in the network structures during aging. Photoelastic Stress Analysis is adopted to monitor the evolution of stresses on rectangular beam samples during absorption and desorption of water. Correlation of water uptake, dynamic mechanical behaviour and transitory stress fields, has allowed to make some assumptions about the influence of the epoxy network on the swelling behaviour.

1. Introduction

Thermoset resins are widely used as matrices for composites, adhesive bonding or coating materials in structural applications. Solvent uptake is a natural and common aging process for such thermosets, leading to a change of thermal resistance (Glass Transition Temperature, T_g) and mechanical behaviour (strength, toughness, etc …), and to the development of internal stresses caused by the swelling action of the absorbed solvent [1]. These changes can have a severe influence on highly constrained structures presenting interfaces between materials with strong properties mismatches (e.g. matrix/fibre interfaces, structural hybrid joints, etc.).

Studies so far have evidenced the presence of many concurrent phenomena influencing the diffusion kinetics and the amount of absorbed water at equilibrium in epoxy based resins. It is commonly accepted that the absorbed water is in part filling the free volume (free water) and in part chemically reacting with the epoxy network forming polar bonds (bonded water) [2–4]. The relative amount of bonded and free water and the role of each type of water in both swelling and degrading phenomena is though much more complex to establish. This is due to the mutual influence of various factors. In fact the formation of bonded water may change the network structure, and in particular its flexibility and free volume [5]. All these effects lead to a final modification in the properties of the aged material difficult to predict [6].

Water diffusion can influence structural properties of the material such as its T_g, which generally decreases with water uptake, and fracture toughness [7,8]. These changes are primarily associated to a plasticization of the material as extensively reported in the literature [1,8–12].

Among the transformations activated by water absorption, one particularly difficult to assess is swelling. Such hydrostatic volume change is usually proportional to the amount of absorbed water. During the transitory from water ingress to saturation a non-uniform distribution of water is responsible for the development of internal stresses, due to non-uniform swelling. Only a few works have attempted the evaluation of such transitory stages, due to the intrinsic difficulty to make an effective full field evaluation of the stress/strain fields [13,14]. Recently the authors have proposed a

* Corresponding author.
E-mail address: giuseppe.pitarresi@unipa.it (G. Pitarresi).

http://dx.doi.org/10.1016/j.polymdegradstab.2016.09.004
0141-3910/

new approach to evaluate the transitory swelling stresses arising during absorption/desorption, which uses Photoelastic Stress Analysis [1]. The method has proven to be robust and easy to implement on transparent and birefringent resin systems, providing a very high sensitivity, sufficient to detect swelling stresses arising also in small sample coupons. The authors have also successfully used the method to investigate the influence of swelling stresses on cracked materials, and to interpret the influence of hydrothermal aging on the material fracture toughness [15,16].

The present work exploits the Photoelastic technique to correlate the evolution of swelling stresses with the network structure of glassy polymers. Two highly crosslinked epoxy resin systems based on DGEBA and DGEBF monomers respectively are compared. These resin systems have been cured with amine DDS, achieving different values of T_g. By analysing the evolution of swelling stresses during absorption and desorption, it has been found that the two considered resin systems achieve a similar stress distribution, with comparable swelling stresses peaks, but the kinetic of the stress evolution is instead different and influenced by the network structure.

2. Experimental procedure

2.1. Materials and sample preparation

The epoxy systems analysed in this work are 2,2-bis[4-(glycidyloxy)phenyl]propane (DGEBA), (epoxide equivalent weight, 172–176, Sigma Aldrich, Italy) and Araldite PY 306 CH (purity almost 100%, Huntsman Advanced Materials, Belgium) based on bis(4-glycidyloxyphenyl)methane (DGEBF); the curing agent is a 4,4′ diamino-diphenyl sulfone (DDS) (Sigma Aldrich, Italy). The chemical formula of the relative monomers are reported in Fig. 1.

The DGEBA and DGEBF resins have been prepared by mixing a stoichiometric amount of DDS to the epoxy at 80 °C, fully dissolved after mechanical stirring for 30 min at 130 °C. The resin blends have then been casted into an aluminium open mould flat plate, having a smooth finish. This made possible to manufacture panels with good thickness control, smooth surface finish and adequate transparency, all necessary features to implement Photoelastic Stress Analysis [1].

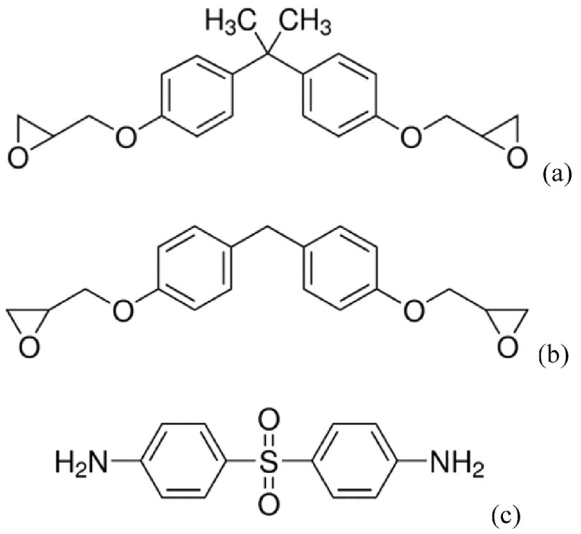

Fig. 1. Molecular structure of monomers DGEBA (a), DGEBF (b) and curing agent DDS (c).

DGEBA and DGEBF based systems have been cured in three steps: the first one consisted of a temperature gradient of 2 °C/min from room temperature to 180 °C, resting at this temperature for 2 h, and cooling at the same rate to room temperature. After this first cure process, beam samples of nominal dimension of 36 × 8 × 3 mm have been cut from the cured panels and post-cured.

In the following the two cured systems will be indicated as DGEBA and DGEBF resins respectively.

The post-curing process has been different for DGEBA and DGEBF resins, due to their different cross-linking network: the former has been post-cured at 200 °C for 2 h followed by a slow cooling to room temperature in 24 h, while the latter has been post-cured at 180 °C for 2 h followed by the same cooling rate applied for DGEBA. The previous treatments were able to provide fully cured and dry samples, without any significant residual stresses left from sample cutting and ambient humidity absorption.

2.2. Hydrothermal conditioning

Hydrothermal aging has been carried out in two baths of deionized water at controlled temperature of 50 °C and 80 °C. Desorption has been performed at room temperature in a recipient with a calcium chloride salt to assure a dry airborne environment. Samples aged at 80 °C have been also subjected to the desorption process.

2.3. Gravimetric and dynamical-mechanical-thermal analysis

The specimens have been taken out of the bath at short time intervals, shorter in the initial stages of absorption and desorption. The samples have then been wiped off of surface water and, after a sufficient time to reach thermal equilibrium with the ambient, weighted on a 10^{-5} g resolution electronic balance. Results have been plotted in terms of percentage of mass uptake M_r versus time t, according to the follow equation:

$$M_r(t) = \frac{M(t) - M(0)}{M(0)} \quad (1)$$

where $M(t)$ is the weight at the time t, $M(0)$ is the initial weight before the hydrothermal aging.

The gravimetric analysis, in the absorption and desorption process, has been carried out until it was not observed a significant mass change.

The glass transition temperature, T_g, has been determined by Dynamical Mechanical Thermal Analysis (DMTA), performed on a Rheometrics DMTA V in a single cantilever beam arrangement at a heating rate of 10 °C/min, frequency of 1.8 Hz and elongation of 0.02%. The temperature corresponding to the tanδ curve peak has been assumed as the value of T_g.

DMTA has been carried out for each hydrothermal conditioning, at four different stages of aging:

1) initial not aged post-cured samples;
2) under maximum swelling stresses, as detected by photoelasticity;
3) at saturation (water uptake equilibrium);
4) at desorption equilibrium (for systems aged at 80 °C).

2.4. Photoelastic stress analysis

The photoelastic technique is able to reveal the average distribution of hygroscopic in-plane stresses arising in the sample, when

this is transparent and birefringent. A quantitative evaluation of the in-plane stress components is in particular performed in this work, by implementing the Tardy Phase Shifting Method (TPSM), described in Refs. [1,17], during the absorption and desorption process.

The photoelastic constant C of the materials has been evaluated on samples with nominal dimension of 90 × 14 × 3 mm, more suitable for a four point bending loading calibration scheme carried out in a circular polariscope in monochromatic light. The photoelastic constant has been evaluated by calibration [1] at the initial condition, before the start of hydrothermal aging, resulting: $C_A = 6.5 \cdot 10^{-5} mm^2/N$ for DGEBA, and $C_F = 7.3 \cdot 10^{-5} mm^2/N$ for DGEBF. The Photoelastic calibration has been repeated on the same beam samples at their water-uptake saturation conditions. This second calibration revealed a negligible influence of aging on the photoelastic constants. The influence of temperature on the material photoelastic constant is instead not an issue since all photoelastic acquisitions have been taken after the samples had reached equilibrium with room environment. This was achieved after about one minute from extraction from the bath, as verified by an Infrared Thermocamera measuring the sample temperature evolution [17].

The photoelastic analysis has been performed throughout the aging conditioning by taking the samples off the conditioning environment (water bath or dry airborne desiccator). During each acquisition, the specimens were left out of the conditioning environment for at most few minutes, and placed in a circular polariscope in monochromatic yellow light (wavelength $\lambda = 589$ nm) to acquire the photoelastic images according with the TPSM procedure. The stresses have been evaluated along the y-axis of symmetry from the edge ($y/W = 0$) to the centre ($y/W = 0.5$) of the sample, being W the total width of the specimen and y the point of analysis, as represented in Fig. 2. The stress function that is obtained with the TPSM analysis is the difference of principal stresses $(\sigma_1\text{-}\sigma_2)$ along the vertical symmetry axis. Due to the beam-shape of the sample, and hence the high length to width aspect ratio, the normal stress component along the y direction is negligible, so it is possible to consider at a first approximation that $(\sigma_1\text{-}\sigma_2)=(\sigma_x\text{-}\sigma_y) \approx \sigma_x$ [1,17]. The isochromatic fringes in the Region Of Interest (ROI), evidenced in Fig. 2, are horizontal which means that each vertical section within the ROI has the same distribution of σ_x.

3. Results and discussion

3.1. Properties before aging

Results of DMTA on the post-cured systems before initiation of aging indicate a T_g of 226 °C for DGEBA and 202 °C for DGEBF. This characterises DGEBA as a system with a generally higher crosslink density than DGEBF. Such statement compares well with findings on similar systems in the literature [18]. It is interesting to quote here also the results of a *Mode I Fracture Toughness* characterisation performed on the same systems in accordance with the ASTM D5056 standard [15,16]. The values of the Mode I Critical Stress Intensity Factor K_{IC} found are: 0.57 MPa*$\sqrt{m}$ for DGEBA and 0.64 MPa*$\sqrt{m}$ for DGEBF. Therefore, DGEBA is more brittle than DGEBF and this is in accordance with its lower network mobility established by DMTA.

3.2. Water uptake

The gravimetric curves during absorption and desorption are reported in Fig. 3a–b. In particular, for the desorption process, carried out only for the system aged at 80 °C, the mass change is normalised by the equilibrium mass uptake (i.e. the relative mass uptake), as Fig. 3b shows. All curves report the average value measured on three nominally identical samples. The standard deviation of all measured weights never exceed the 4% of the respective average weight, indicating a low dispersion.

For both aging temperatures, it is found that DGEBA absorbs more water than DGEBF, although the gap seems to decrease at 80 °C. This is believed to be related to the higher crosslink density of DGEBA. Such higher density determines an intrinsically smaller chain mobility, which is by some authors usually associated to a less compact system, and hence to a higher free volume [5,11,12,19]. With temperature increase, the more flexible DGEBF network is probably more sensitive to the increased kinetics of water absorption, and this can provide an explanation for the reduction of the gap with DGEBA in absorbed water. Another noteworthy feature of Fig. 3a is the crossing of the DGEBA 50 °C curve with the DEGBA 80 °C curve, with a final equilibrium water absorption at 50 °C slightly higher than the 80 °C. A similar behaviour is also reported in Ref. [20] for similar DGEBA-DDS systems. As demonstrated by Ref. [21], and mentioned by Ref. [20], the lack of correlation between the equilibrium water content and the aging temperature is a likely occurrence with systems with a medium polarity, such as the epoxies of this work.

The diffusion coefficient D (diffusivity) [22] for the two studied epoxy systems is reported in Table 1, calculated by the Fick's second law, assuming the last monitored values of water uptake as representative of the equilibrium condition.

The samples aged at 80 °C have been also subject to a controlled desorption process immediately following the end of absorption. Desorption has been monitored for 2800 h, i.e. up to the formation of a consolidated plateau trend in the relative mass change curve (see Fig. 3b). It is noteworthy to observe the presence of a residual water content at the plateau, which amounts to about 52% and 38% of the water content at saturation, for DGEBF and DGEBA respectively. From Fig. 3b it is also observed that DGEBA has an initial faster desorption rate. Since the desorption process has been carried out at a room temperature, activated only by an external controlled dry airborne environment, it is assumed that the desorbed water is mainly free water.

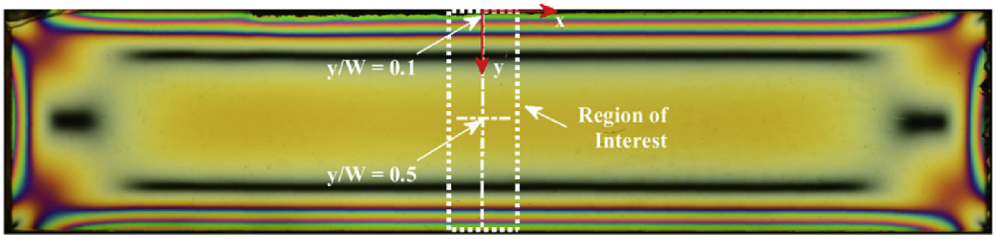

Fig. 2. Isochromatic map of the whole sample acquired in a white light dark field polariscope.

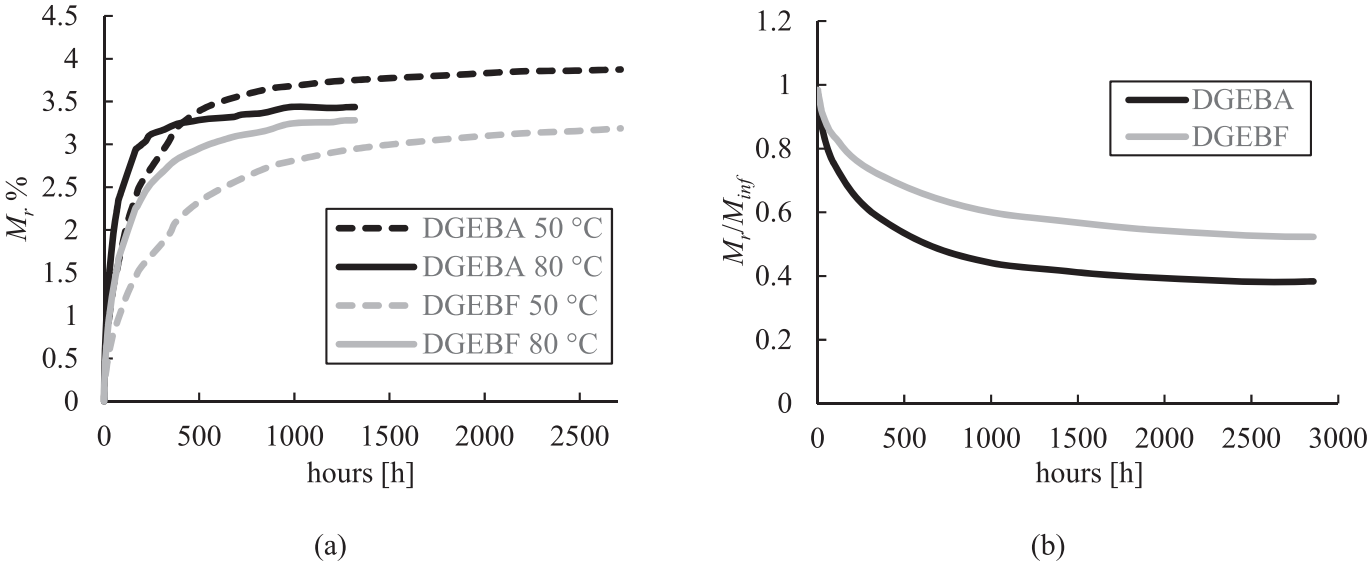

Fig. 3. Gravimetric curves: (a) absorption; (b) desorption.

Table 1
Diffusivity for DGEBA and DGEBF at different temperatures of hydrothermal aging.

Material	Diffusivity at 50 °C [10^{-8} cm^2/s]	Diffusivity at 80 °C [10^{-8} cm^2/s]
DGEBA	0.93	2.83
DGEBF	0.58	1.71

3.3. Dynamic mechanical thermal analysis

DMTAs have been performed at four stages (see Section 2.3). In particular, stage 2 is indicative of a situation where the sample is experiencing significant internal swelling stresses. These transient swelling stresses have the highest traction value at the sample centre ($y/W = 0.5$) and compression value on the sample edge ($y/W = 0$). The time at which these stresses reach a maximum is different for the two materials (DGEBA or DGEBF) and for the two aging bath temperatures (50 °C or 80 °C).

DMTA results are reported in Fig. 4. The peak in the tanδ curves is related to the relaxation of the cross-linked network clusters and the temperature is taken as the T_g. Table 2 reports results from the DMTA in terms of T_g and the corresponding tanδ value. For tanδ curves showing more than one peak, the value of each peak is reported.

In an attempt to find a correlation between the DMTA behaviour and the gravimetric data, some assumptions can be made about the role of free volume in the two studied systems. The free volume consists of permanent cavities, inside a covalently formed network, which in turn can include physical networks due to Van der Waals interactions among the molecular chains forming the same permanent cavities [5]. Moreover, the extension of this phenomenon is strictly related to both chains mobility and polarity. The permanent network is responsible of the T_g of the material, while the whole network governs the initial uptake. Some authors have suggested that a smaller crosslinking density, e.g. witnessed by a lower T_g, is generally associated to smaller free volume (due to the collapsing of the flexible network chains), probably determined by an increased mobility of the chains of the physical network [18,19]. This would explain why DGEBF is absorbing less water than DGEBA, and with a lower diffusion rate (Fig. 3a).

With the progression of water uptake, the tanδ curve is always shifted towards lower temperatures and it is common to observe a broadening of the curve and the formation of other peaks or shoulders.

For the stressed ageing condition (i.e. maximum stress, stage 2), at both 50 °C and 80 °C, it is observed that the T_g value is only slightly affected in DGEBA, while it significantly decreases in DGEBF, even if the tanδ curve shows always a broadening of the peak.

DMTA performed at the end of the absorption period (i.e. at saturation) shows a significant T_g reduction in both systems with also the occurring of two peaks. This modification suggests that the water absorption induces the formation of heterogeneities in the cross-linked networks, with the occurring of plasticization/degradation phenomena. In particular, DGEBF shows a larger decrease than DGEBA, with similar intensity of the two peaks at 50 °C and a prevalence of the first one at 80 °C, while DGEBA always shows a prevalence of the second peak on the first one.

Looking at the water uptake curves at both 50 °C and 80 °C it can be observed that the decrease of T_g is always higher in DGEBF than in DGEBA, at all ageing absorption conditions despite the lower water uptake of DGEBF. This is to be referred to the less dense starting network of DGEBF, which induces a higher sensibility to plasticization effects.

DMTA performed at the end of the desorption period (after ageing at 80 °C) shows a tendency of both materials to recover the initial T_g. It is though observed that the DGEBF peak remains quite far away from the initial position with a residual T_g of 171 °C against 202 °C of the unaged system, indicating a persistence of plasticization effects. Instead, the DGEBA system is able to almost fully recover the unaged T_g. Indeed from gravimetric data (see Fig. 3b) both DGEBA and DGEBF show a residual water content at the desorption plateau, with a higher value for DGEBF, which could explain its lower ability in recovering the virgin T_g under desorption. The higher amount of desorbed water exhibited by DGEBA could then indicate that this system has a higher free volume with a higher amount of free water, as already hypothesized elsewhere on the basis of its higher crosslink density [23].

3.4. Photoelastic stress analysis

Concentration of water during the initial stages of absorption is not uniform in the sample. Only when the gravimetric curve

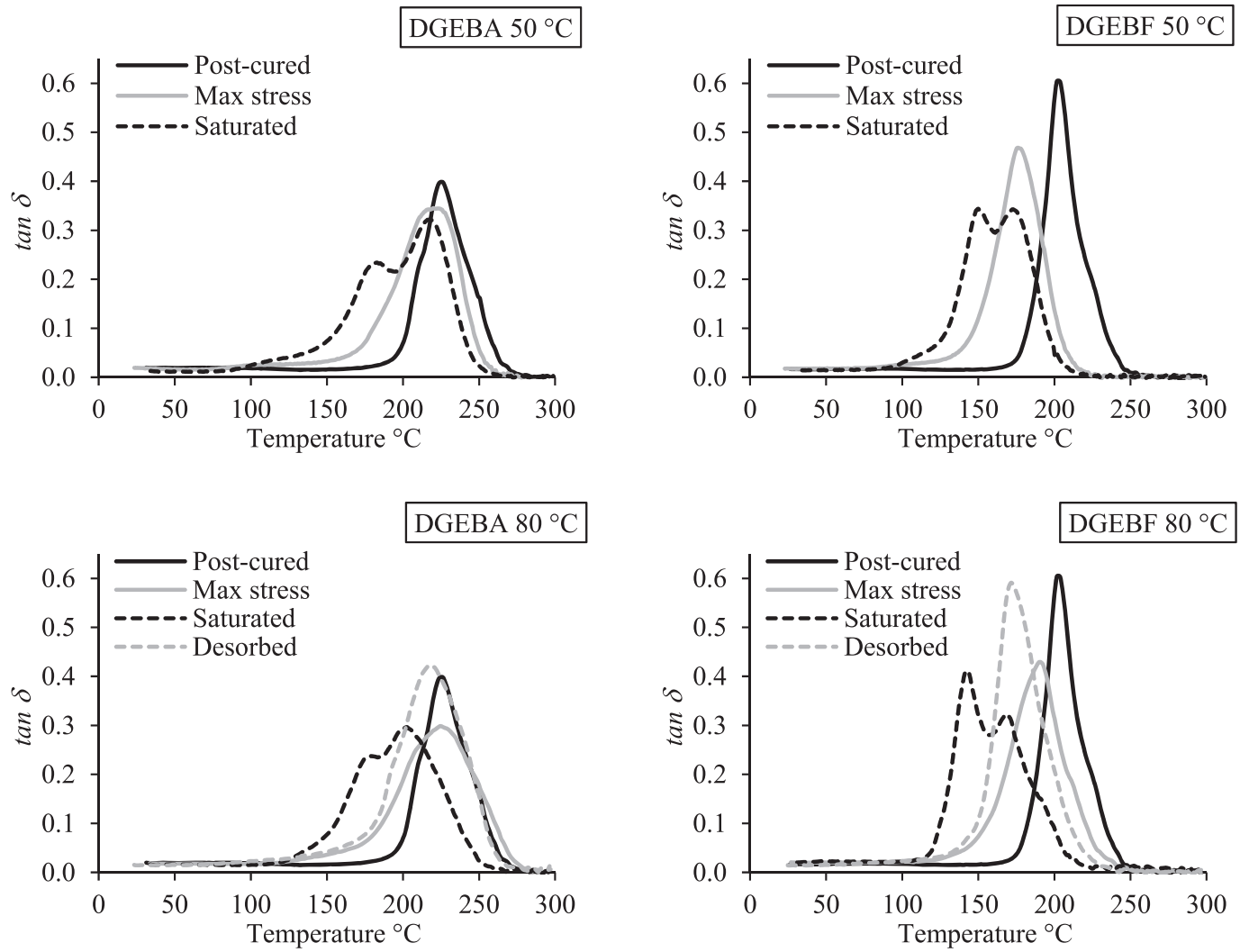

Fig. 4. DMTA curves for DGEBA and DGEBF systems.

Table 2
Glass transition temperatures and tanδ values at different stages of hydrothermal aging for DGEBA and DGEBF.

	DGEBA		DGEBF	
	T_g [°C]	*tanδ*	T_g [°C]	*tanδ*
Post-cured	226	0.40	202	0.60
50 °C – max stress	223	0.34	176	0.47
80 °C – max stress	225	0.30	190	0.43
50 °C – saturated	181–218	0.23–0.32	150–173	0.34–0.34
80 °C – saturated	179–202	0.24–0.30	142–168	0.41–0.32
80 °C – desorbed	217	0.42	171	0.59

establishes its plateau, a uniform equilibrium water concentration is hypothetically achieved (at saturation). During the absorption process, the non-uniform water concentration gives rise to a non-uniform swelling in the sample. This swelling is usually modelled as a hydrostatic strain filed, where normal strains are proportional to water content through a Coefficient of Hygroscopic Swelling [24]. Then non-uniform swelling is a side effect of transitory non-uniform water concentration, and it determines an internal stress field that must be self-equilibrated.

3.4.1. Evolution of swelling stresses: general features

Photoelastic Stress Analysis is able to measure the average in-plane stress components induced by such non-uniform swelling/concentration [1]. Fig. 5 shows the isochromatic maps in white light [17] in the ROI (see Fig. 2). These isochromatics have been acquired at different instants of the absorption process, going from initial to saturation stage. The colours of the isochromatic fringes codify a value of σ_x. A quantitative evaluation of σ_x is given in Fig. 6, obtained with the TPSM recalled in section 2.4. Fig. 6 plots σ_x along the semi-width segment going from the edge ($y/W = 0$) to the centre ($y/W = 0.5$). Two curves are in particular reported, one referred to the instant of maximum peak stress during absorption, and one to the maximum stress during desorption. The location where the stress is zero in Fig. 6 corresponds to the position of the fringe coloured black in Fig. 5. It is found that during absorption process the zones between the black fringes and the sample edges are in prevalent compression ($\sigma_x < 0$), and the zone between the two black fringes is in traction ($\sigma_x > 0$), as Fig. 6 indicates. This finding has a direct physical interpretation, i.e. the inner material is initially un-swelled while the outer material starts to swell. Therefore, the inner material acts as an internal constraint for the expansion of the outer material, which then develops a compression stress. The inner material counter develops a traction in order also to maintain such

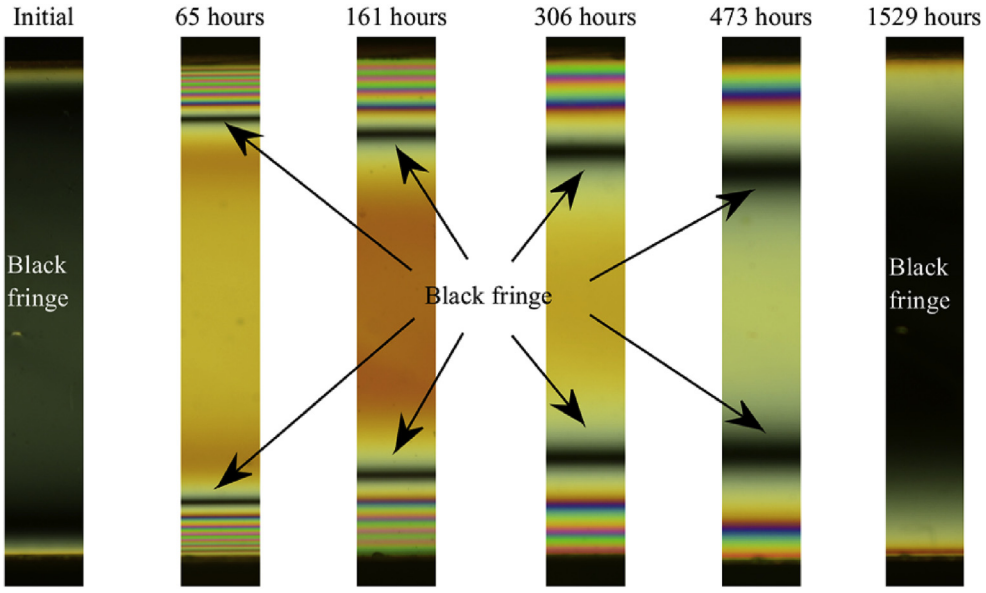

Fig. 5. Evolution of the isochromatic fringes of DGEBA during absorption at 50 °C, obtained in a circular dark field polariscope in white light.

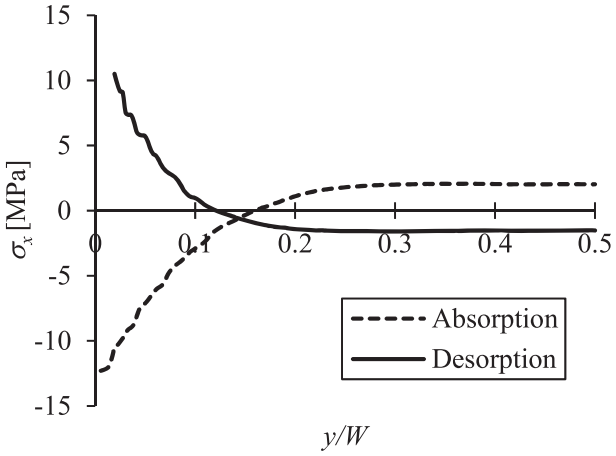

Fig. 6. DGEBA maximum swelling stresses during absorption at 80 °C and desorption.

internal stresses self-equilibrated.

Fig. 5 shows also that the higher stresses at the border and in the centre are reached at relatively early stages from initiation of aging conditioning. In fact, comparing the images at 65, 161 and 306 h the number of fringes between the border and the black fringe is progressively reduced, indicating a relaxation of stresses. Hence, σ_x reaches a peak at the sample edge, and then evolves toward a progressive reduction. This relaxation is almost complete in the image taken at 1529 h. The reason for such evolution is related with the kinetics of water diffusion. While water gains its ingress in the inner zones of material, swelling is extended to these zones. A more extended swelling reduces the internal constraint and thus the stresses. When the swelling becomes uniform due to a complete water uptake of the whole sample, this also becomes fully relaxed. The final stress free condition does not mean un-strained. In fact, the sample is swelled uniformly.

During desorption a similar behaviour is observed although inverted in terms of swelling stresses. In fact, the outer zones of material start to release the absorbed water more rapidly. They then un-swell faster than the inner material, and are hence loaded in traction ($\sigma_x > 0$) due to the arising internal constraint. This brings to a situation where the internal swelling stresses, arising during desorption, are opposite to those developed under absorption, as shown in Fig. 6.

3.4.2. Evolution of swelling stresses: comparison of systems

A quantitative analysis of swelling stresses versus time has been performed on the *y*-axis of symmetry, and in particular along the segment going from the edge to the centre (see Fig. 2). The curves of σ_x versus time, shown in Fig. 7, are referred to two points in particular: one near the edge, $y/W = 0.1$, and one at the centre, $y/W = 0.5$.

It is observed that the swelling stress curves have a similar trend in both DGEBA and DGEBF, and for both 50 °C and at 80 °C aging temperatures. The maximum stresses in the two observed points are reached relatively soon compared to the total time required to reach saturation. At this regard, it is observed that curves in Fig. 7 are interrupted earlier than the total time to saturation, to better appreciate the interval of swelling stress development. From Fig. 7 it is also found that the centre point remains always in traction, $\sigma_x > 0$, and the stress tend to zero slowly with time after reaching a peak at around 2 MPa. The part of sample in compression is smaller than the part in traction, so the compression stresses have to reach higher absolute values to preserve self-equilibrium.

It is noticed also that the position of the black fringe y_0 relative to the sample width W is similar when DGEBA and DGEBF reach their respective traction/compression peak stresses. This is shown in Fig. 8 for the 50 °C aging case, and summarised in Table 3 for all cases.

While the general trend and peak values of swelling stresses are similar in both DGEBA and DGEBF, the most noteworthy difference arising from Fig. 7 lies in the evolution of stresses with time. It is in fact well noticeable that DGEBF has a slower kinetics, with smaller gradients characterising the swelling stresses evolution. This tendency is also reproduced at both aging temperatures. The conclusion from this comparison is that the two materials achieve similar maximum swelling stresses, but with different kinetics. The kinetic of swelling stress development follows that of water diffusion, so DGEBF is slower in diffusing water and in reaching the maximum swelling stresses. The more severe decrease of glass transition

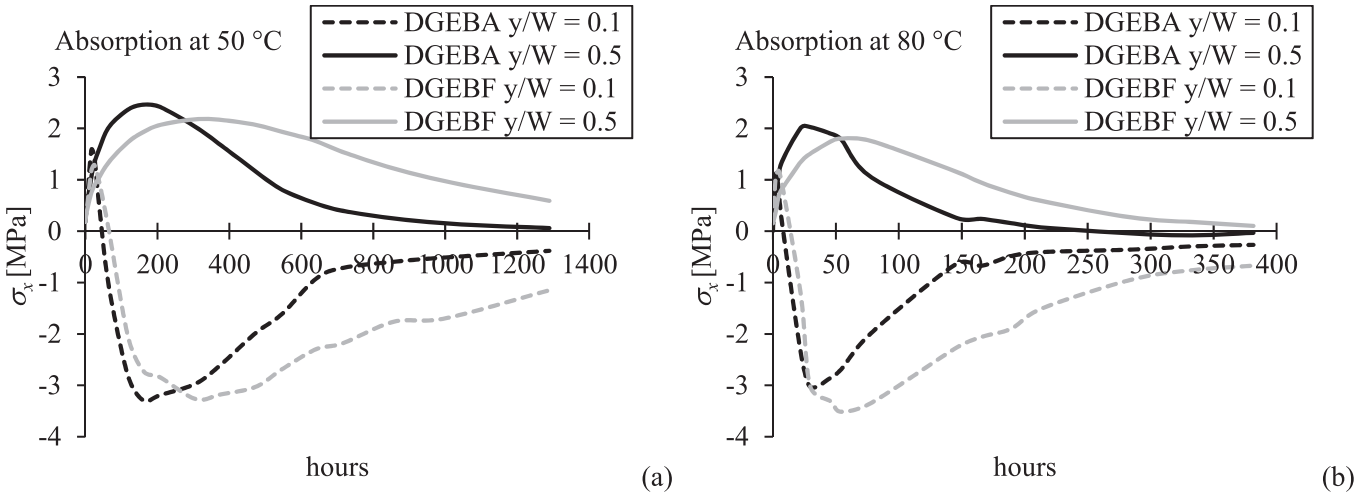

Fig. 7. Stress curves at the edge and at the centre of specimen for DGEBA and DGEBF at 50 °C (a) and 80 °C (b).

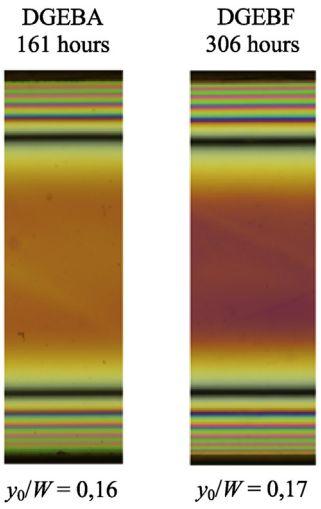

Fig. 8. Relative black fringe position y_0/W at maximum swelling stress at 50 °C.

Table 3
Mass uptakes and black fringe position at the time of maximum swelling stress detected at $y/W = 0.5$

Material	DGEBA		DGEBF	
Aging temperature	50 °C	80 °C	50 °C	80 °C
Max stress time	161 h	30 h	306 h	54 h
Black fringe position y/W	0.16	0.16	0.17	0.18
M_r	2.35%	1.55%	1.92%	1.39%
M_r/M_{inf}	0.61	0.45	0.61	0.43

The influence of desorption on swelling stresses was investigated on the samples previously saturated at 80 °C.

temperature exhibited by DGEBF with aging is related with a reduction of cross-link density that could foster a further compacting of the free volume [19]. If this rationale is true, than the ingress of water in the kernel of the sample becomes more difficult with aging time, and this can be one reason for the persistence of high swelling stresses and their slower relaxation gradient.

Gravimetric and Photoelastic data have been directly correlated by plotting swelling stresses versus the relative mass uptake, i.e. the ratio of actual water uptake to the final water uptake at saturation: M_r/M_{inf} (see Fig. 9 and Table 3).

Curves in Fig. 9 for the $y/W = 0.1$ show that in this point a traction stress is initially developed, which then gradually evolves to a compression stress. This is due to the fact that this point is crossed by the neutral axis during water diffusion, so initially it is on the side of traction stresses and after a certain mass uptake it falls on the side of compression, which reaches a maximum and then goes back to zero (final relaxation phase). This behaviour is present also in Fig. 7, although the part on the curve in traction is very close to the vertical y-axis and evolves very rapidly to a compression.

One noteworthy outcome from curves in Fig. 9 is that all stress peaks seem to occur at similar values of relative mass uptake. Then, while both the absolute mass uptake and maximum stress values in the two DGEBA and DGEBF systems exhibited a different behaviour when looked against time (see also Table 3), the maximum stress values are instead falling at about the same relative mass uptake. This occurrence is found in both the two observed points, i.e. at the centre and near the edge. Furthermore, it is also observed that the peaks in the 50 °C aging are slightly shifted towards higher relative mass uptakes compared to 80 °C aging. Hence, a system aging at lower temperature employs a higher fraction of water of the total amount absorbed, to develop the swelling stress peaks.

Fig. 10 shows the plot of the stresses versus desorption time. It is noteworthy to confirm that σ_x is now negative (compression) in the centre, and positive (traction) in the border zone. This traction in the outer zones of the sample surface might be dangerous when small edge cracks are present. In fact, in this case the un-swelling stresses would develop a Mode I opening loading of such defects.

Fig. 10 shows that stress evolution in DGEBF and DGEBA is initially similar. Soon after the reach of the first peak, DGEBF starts to develop a slower rate of stress relaxation compared to DGEBA, in analogy to what observed during absorption. While DGEBA is able to relieve almost completely its stresses during the observation time (about 3500 h), DGEBF remains significantly stressed.

Fig. 11 shows the curves of stress versus loss of relative mass uptake for the centre point ($1\text{-}M_r/M_{inf}$).

Contrary to what observed with absorption, in Fig. 11 the curves relative to the two materials now seem to have a more distinguished evolution. The peak in DGEBF is reached at a value of loss of relative mass uptake slightly higher than DGEBA. It is interesting to recall here the results of DMTA, which showed a different ability of the two materials to recover their T_g at the end of desorption. In

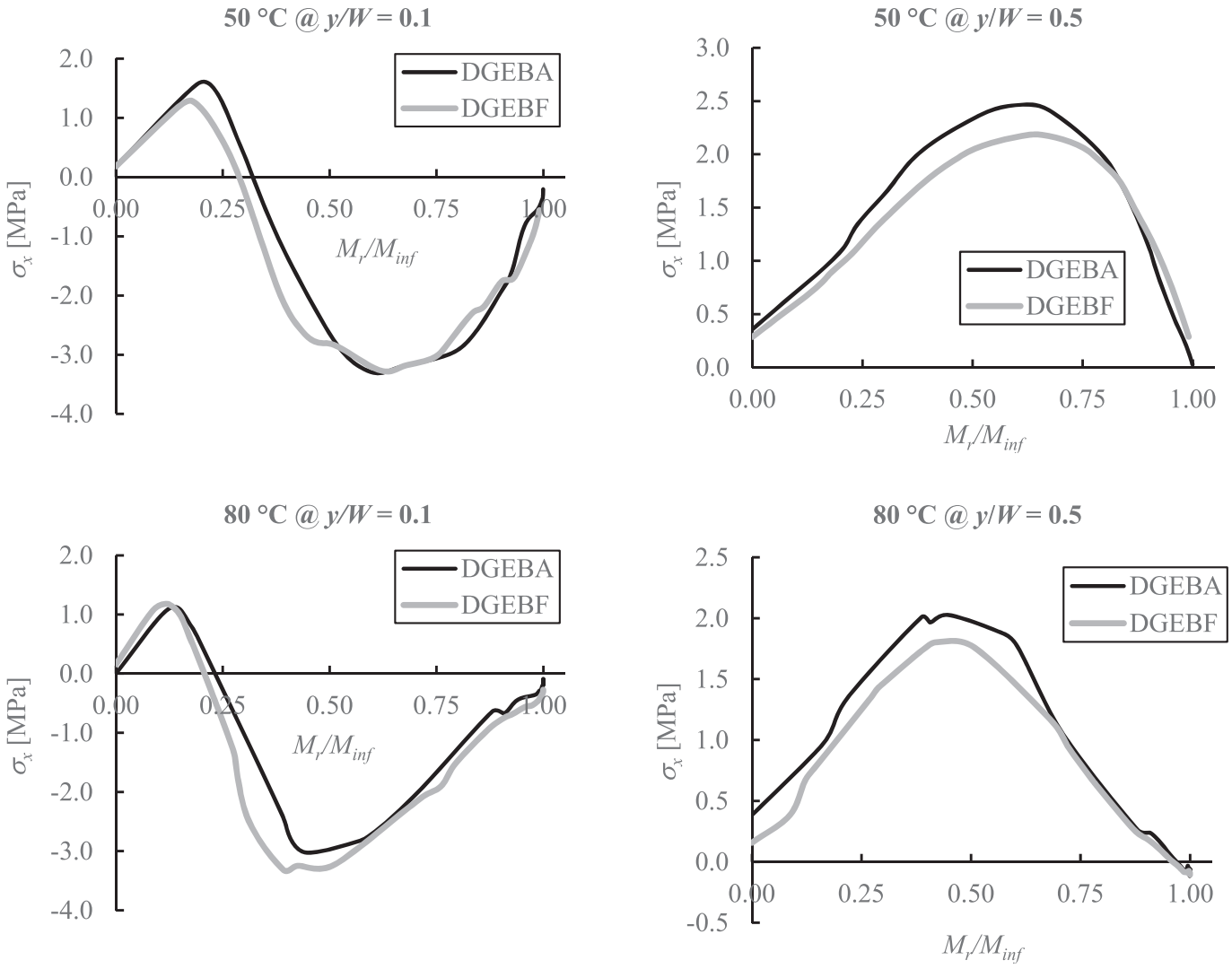

Fig. 9. Plots of swelling stresses versus the relative mass uptake M_t/M_{inf}.

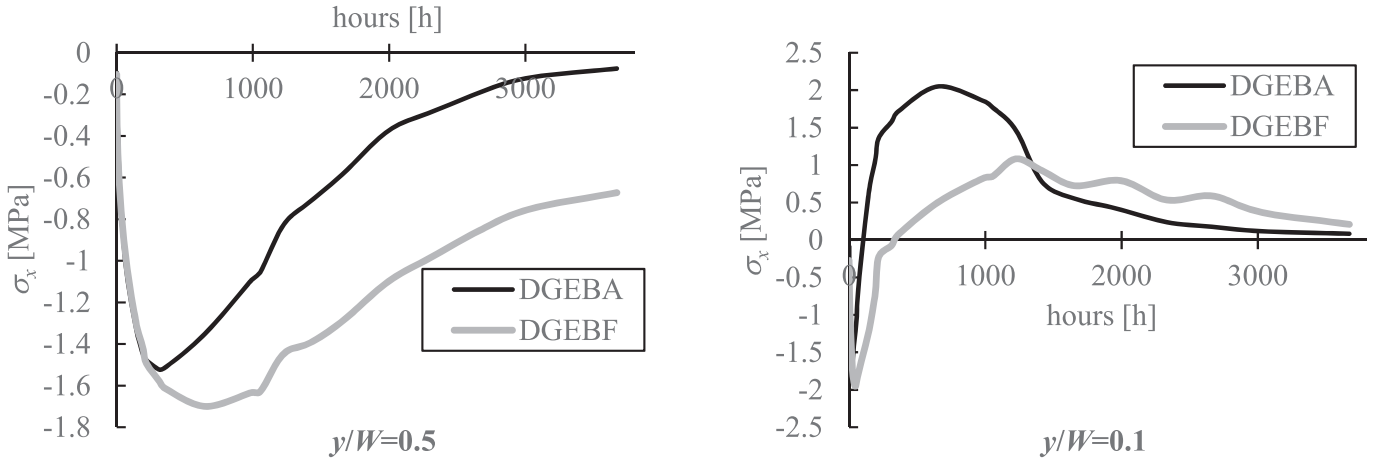

Fig. 10. Swelling stress curves during the desorption process of systems previously saturated at 80 °C.

particular, the T_g of DGEBF remained significantly lower than the unaged value. This might determine a situation that hampers the release of water and slows down the relaxation of stresses, as shown in Fig. 10.

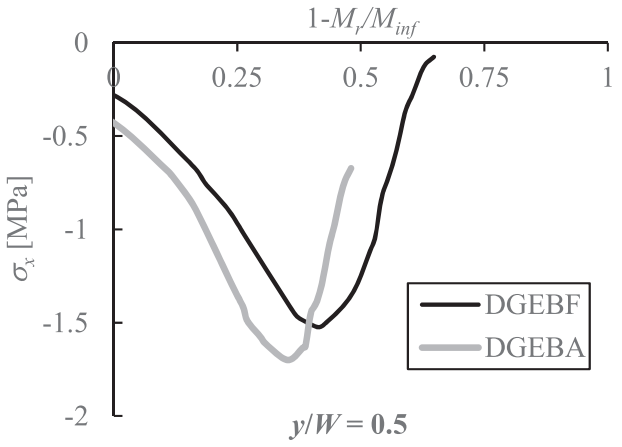

Fig. 11. Stress versus loss of relative mass uptake at the centre point during desorption.

4. Conclusion

The present work proposed a photoelastic study to investigate the rate of stresses arising during hydrothermal swelling, and to correlate this phenomenon with both the diffusion kinetics and network structure of two highly cross-linked epoxy resins, based on DGEBA and DGEBF.

The initial tests on unaged systems showed that DEGBA has a higher cross-linking density than DGEBF. During hydrothermal ageing at two different temperature values, the absorption curves indicated for DGEBA both a higher diffusivity and water uptake at both temperatures, suggesting the formation of a higher free volume in DGEBA. Moreover, DMTA analysis showed plasticization/degradation phenomena in both systems evidenced by both a general shift of the tanδ curves towards lower temperatures and the formation of different relaxation peaks, with a marker effect on DGEBF due to its lower starting cross-linking density.

The measured swelling stresses during absorption have reached similar trends and peak values in both systems, and at both aging temperatures, indicating a low sensitivity of these values with the amount of absorbed water. The evolution of stresses with time has instead revealed some differences. DGEBF in particular exhibits a slower kinetic of formation and evolution of swelling stresses. This is believed to be correlated with the slower kinetic of water diffusion deriving from the lower cross-linking density of this system, as compared to DGEBA.

An interesting outcome of the work has regarded the correlation of swelling stresses with the relative mass uptake M_t/M_{inf}. The curves in this case were almost overlapping for both DGEBA and DGEBF, at both aging temperatures. This result suggests that the transient nature of swelling stresses is primarily related to the actual proportion of water uptake with respect to the equilibrium water uptake.

A desorption process at room temperature in a dry airborne has been also investigated. In this case, the nature of the internal constraint is opposite to the case of absorption, with a fast unswelling of the outer zone and a slow evolution of the swelled kernel zone. This determines the arising of traction stresses in the borders of the sample. The drying environment is not able to eliminate all the absorbed water, and the residual relative water uptake at the plateau of the gravimetric curves is higher for DGEBF (about 52%) than for DGEBA (about 38%), suggesting a higher amount of free water for the last system. DGEBA also exhibits an almost complete recovery of the original T_g. The Photoelastic analysis revealed that DGEBA is faster in relaxing the developed internal stresses, which are almost completely relaxed at the reach of the plateau. On the contrary, DGEBF has a slow evolution of stress relaxation, which could be related to the persistence of a low T_g and a higher residual relative mass uptake.

References

[1] G. Pitarresi, M. Scafidi, S. Alessi, M. Di Filippo, C. Billaud, G. Spadaro, Absorption kinetics and swelling stresses in hydrothermally aged epoxies investigated by photoelastic image analysis, Polym. Degrad. Stab. 111 (1) (2015) 55–63.
[2] P.S. Theocaris, E.A. Kontou, G.C. Papanicolaou, The effect of moisture absorption on the thermomechanical properties of particulates, Colloid & Polym. Sci. 261 (1983) 394–403.
[3] G.Z. Xiao, M.E.R. Shanahan, Water absorption and desorption in an epoxy resin with degradation, J. Polym. Sci. Part B Polym. Phys. 35 (1997) 2659–2670.
[4] J. Zhou, J.P. Lucas, Hygrothermal effects of epoxy resin. part I: the nature of water in epoxy, Polymer 40 (20) (1999) 5505–5512.
[5] S. Alessi, E. Caponetti, O. Güven, M. Akbulut, G. Spadaro, A. Spinella, Study of the curing process of DGEBA epoxy resin through structural investigation, Macromol. Chem. Phys. 216 (5) (2015) 538–546.
[6] M.R. VanLandingham, R.F. Eduljee, J.W. Gillespie Jr., Moisture diffusion in epoxy systems, J. Appl. Polym. Sci. 71 (5) (1999) 787–798.
[7] P. Nogueira, C. Ramírez, A. Torres, M.J. Abad, J. Cano, J. López, I. López-Bueno, L. Barral, Effect of water sorption on the structure and mechanical properties of an epoxy resin system, J. Appl. Polym. Sci. 80 (1) (2001) 71–80.
[8] S. Alessi, D. Conduruta, G. Pitarresi, C. Dispenza, G. Spadaro, Accelerated ageing due to moisture absorption of thermally cured epoxy resin/polyethersulphone blends. Thermal, mechanical and morphological behaviour, Polym. Degrad. Stab. 96 (4) (2011) 642–648.
[9] L. Nunez, M. Villanueva, F. Fraga, M.R. Nunez, Influence of water absorption on the mechanical properties of a DGEBA (n=0)/1, 2 DCH epoxy system, J. Appl. Polym. Sci. 74 (1999) 353–358.
[10] Y.C. Lin, X. Chen, Moisture sorption–desorption–resorption characteristics and its effect on the mechanical behavior of the epoxy system, Polymer 46 (2005) 11994–12003.
[11] O. Starkova, S. Chandrasekaran, L.A.S.A. Prado, F. Tölle, R. Mülhaupt, K. Schulte, Hydrothermally resistant thermally reduced graphene oxide and multi-wall carbon nanotube based epoxy nanocomposites, Polym. Degrad. Stab. 98 (2) (2013) 519–526.
[12] O. Starkova, S.T. Buschhorn, E. Mannov, K. Schulte, A. Aniskevich, Water transport in epoxy/MWCNT composites, Eur. Polym. J. 49 (8) (2013) 2138–2148.
[13] G.M. Odegard, A. Bandyopadhyay, Physical aging of epoxy polymers and their composites, J. Polym. Sci. Part B Polym. Phys. 49 (24) (2011) 1695–1716.
[14] M.B. Jackson, S.R. Heinz, J.S. Wiggins, Fluid ingress strain analysis of glassy polymer networks using digital image correlation, Polym. Test. 31 (8) (2012) 1131–1139.
[15] G. Pitarresi, A. Toscano, M. Scafidi, M. Di Filippo, S. Alessi, G. Spadaro, Photoelastic stress analysis assisted evaluation of fracture toughness in hydrothermally aged epoxies, Frat. Ed. Integr. Strutt. 30 (2014) 127–137.
[16] S. Alessi, M. Di Filippo, G. Pitarresi, M. Scafidi, A. Toscano, Fracture toughness of hydrothermally aged epoxy systems with different crosslink density, Procedia Eng. 109 (2015) 507–516.
[17] M. Scafidi, G. Pitarresi, A. Toscano, G. Petrucci, A. Alessi, A. Ajovalasit, Review of photoelastic image analysis applied to structural birefringent materials: glass and polymers, Opt. Eng. SPIE 54 (8) (2015).
[18] K. Frank, J. Wiggins, Effect of stoichiometry and cure prescription on fluid ingress in epoxy networks, J. Appl. Polym. Sci. 130 (1) (2013) 264–276.
[19] M.B. Jackson, M. Kaushik, S. Nazarenko, S. Ward, R. Maskell, J. Wiggins, Effect of free volume hole-size on fluid ingress of glassy epoxy networks, Polymer 52 (2011) 4528–4535.
[20] L. Li, Y. Yu, Q. Wu, G. Zhan, S. Li, Effect of chemical structure on the water sorption of amine-cured epoxy resins, Corros. Sci. 51 (12) (2009) 3000–3006.
[21] I. Merdas, A. Tcharkhtchi, F. Thominette, J. Verdu, K. Dean, W. Cook, Water absorption by uncrosslinked polymers, networks and IPNs having medium to high polarity, Polymer 43 (17) (2002) 4619–4625.
[22] J. Crank, J. The Mathematics of Diffusion, Clarendon, Oxford, 1994 (Chapter 4).
[23] P.J. Flory, Principles of Polymer Chemistry, Cornell University, Ithaca, NY, 1953.
[24] J. Zhou, Transient analysis on hygroscopic swelling characterization using sequentially coupled moisture diffusion and hygroscopic stress modeling method, Microelectron. Reliab. 48 (2008) 805–810.